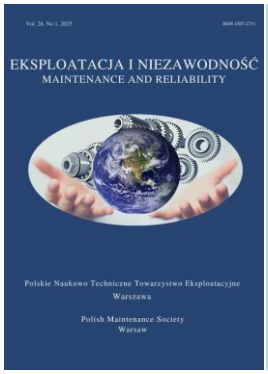

Eksploatacja i Niezawodnosc – Maintenance and Reliability

Volume 27 (2025), Issue 1

journal homepage: http://www.ein.org.pl

Article citation info:
Lei C, Miao C, Yu Y, Wang L, Wang B, Rolling bearing fault diagnosis method based on multi-scale pooling residual convolutional neural network under noisy environment, Eksploatacja i Niezawodnosc – Maintenance and Reliability 2025: 27(1) http://doi.org/10.17531/ein/192167

Rolling bearing fault diagnosis method based on multi-scale pooling residual convolutional neural network under noisy environment

Indexed by: Web of Science Group

Chunli Lei[a], Chengxiang Miao[a,*], Yongqin Yu[b], Lu Wang[a], Bin Wang[a]

[a] Lanzhou university of technology, China
[b] Yunnan Wenshan Aluminum Co, Ltd, China

Highlights

- Wide convolution kernel is used for feature extraction.
- The MSPFE module combined with UPA is proposed.
- Gated convolution and a new activation function IReLU are put forward. On the basis of the ReLU function, the IReLU activation function introduces a new continuous function in the negative half axis to overcome the shortcomings of the existing activation function.

Abstract

To address the issues of unstable performance and poor generalization ability of bearing fault diagnosis model caused by strong noise and variable operating conditions, a novel method based on multi-scale pooling residual convolutional neural network (MSPRCNN) is proposed in this paper. Firstly, by converting vibration signals to frequency domain with Fourier Transform (FT) and utilizing wide convolution kernels for feature extraction, the approach enhances fault detection. Then, a multi-scale pooling feature extraction (MSPFE) module is presented, which captures information at different scales to simplify complexity, while an up-sampling position attention (UPA) module is designed to establish correlations between frequency domain positions. Finally, the MSPRCNN model is built, which employs gated convolution (GC) instead of standard convolution to reduce the impact of noise and solve the problem of vanishing gradient, and the IReLU activation function is put forward to improve model feature representation. Experimental results on two datasets show that the fault recognition accuracy is 98.71% under variable loads and 98.2% under variable speeds. The MSPRCNN model outperforms other methods in fault recognition accuracy and generalization in noisy environments.

Keywords
strong noise, multi-scale pooling, up-sampling, gated convolution, IReLU activation function

1. Introduction

In industrial production, bearings, as key components to support the operation of rotating machinery, play a vital role in the fields of aviation, aerospace and intelligent manufacturing. Their stability and reliability directly affect the efficiency and safety of equipment. Once the bearing fails, it will cause mechanical equipment damage and other consequences. Therefore, it is of great significance to develop an accurate and reliable bearing fault diagnosis method for timely detection, ensuring the normal operation of mechanical equipment and reducing safety risks [1-2].

Traditional rolling bearing fault diagnosis methods usually rely on vibration signal analysis. However, these methods show

(*) Corresponding author.
E-mail addresses: C. Lei (ORCID: 0000-0002-8376-9290) lclyq2004@163.com, C. Miao (ORCID: 0009-0002-1212-8952) 2198074340@qq.com, Y. Yu (ORCID: 0009-0003-9942-2165) yyq037529@163.com, L. Wang (ORCID: 0009-0007-1350-4303) wanglu_314@outlook.com, B. Wang (ORCID: 0009-0001-4086-3121) 401952710@qq.com,

limitations in the face of complex working conditions. For example, in the case of variable operating conditions and strong noise, the traditional method can't accurately identify the characteristics of bearing faults, resulting in missed diagnosis or misdiagnosis [3-4]. Therefore, it is a research hotspot to seek new bearing fault diagnosis methods to cope with the challenges under complex working conditions. In recent years, deep learning (DL), as a powerful data-driven method, has shown excellent performance in many fields. With the development of DL, classical networks such as LeNet-5, AlexNet, VGGNet, Inception, and ResNet have emerged [5-6], and are applied in the field of intelligent fault diagnosis, which provides strong technical support for fault diagnosis. Many scholars have also proposed some new methods, which have achieved remarkable results in improving the accuracy and reliability of fault diagnosis. Zhao et al [7] used signal-to-image mapping (STIM) to convert one-dimensional vibration signals into two-dimensional grayscale images, and then input them into the established convolutional neural network(CNN) model to achieve fault classification. Wu et al [8] adopted continuous wavelet transform (CWT) to convert the original signal into the two-dimensional image, and then input the images into the deep learning model for feature extraction and diagnosis. Zhang et al [9] utilized Gram angle field (GAF) for image coding, and then combined extreme learning machine (ELM) with CNN to realize bearing fault diagnosis. Since the original signal is a 1D time series, converting it into a 2D image will lose some information, and increase the computational complexity and time. Therefore, some scholars have successively proposed one-dimensional CNN models. Xie et al [10] proposed a new one-dimensional convolutional neural network (ODCNN) for rolling bearing fault diagnosis. Hakim et al [11] introduced a one-dimensional convolutional neural network (1D-CNN) for processing frequency-domain signals.

However, for complex multi-dimensional features, a single convolution kernel cannot extract multi-dimensional information from complex vibration signals. Therefore, some scholars have proposed multi-scale CNN for bearing fault diagnosis [12-14]. Lee et al [15] introduced multi-scale residual attention mechanism and multi-channel network (MSCNet) to effectively extract meaningful features from signals of different scales. Kang et al [16] used the multi-scale convolutional neural network (MSCNN)model to effectively extract fault sensitive features. Zhang et al [17] proposed a rolling bearing fault diagnosis method based on adaptive multivariate variational mode decomposition (AMVMD) and multi-scale convolutional neural network (multi-scale CNN) to solve the problem of limited ability of single signal analysis method to identify multivariate data features. Many new CNN methods have addressed some issues in fault diagnosis, however, due to the presence of environmental noise, the diagnosis of bearing faults has become more complex and challenging. Therefore, bearing fault diagnosis in noisy environment has become a new study focus in the current engineering field. In order to solve the problem of noise interference in vibration signals, Peng et al [18] used a multi-branch anti-noise CNN to automatically learn and fuse a large amount of fault information from multiple signal components and time, and then completed the identification of bearing faults. Huang et al [19] proposed an improved label noise robust auxiliary classifier generative adversarial network (rAC-GAN) for fault diagnosis of wind turbine gearbox bearings. Liang et al [20] combined Wavelet Transform (WT) with Improved Residual Neural Network (IResNet) to solve the problem of low accuracy of traditional methods affected by noise interference. Hu et al [21] used EfficientNet to establish a fault diagnosis model, and introduced the attention mechanism to improve the diagnosis accuracy of bearing in complex noise environment.

The activation function is a very important part of the neural network, which makes the neural network model better learn and represent complex data patterns by introducing nonlinear properties. Traditional activation functions such as Sigmoid, ReLU and Tanh can meet the needs of neural networks to a certain extent, but there are also some problems, such as gradient disappearance, gradient explosion and neuron death [22]. In order to solve these problems, researchers have proposed some new activation functions in recent years. Zheng et al [23] proposed a Fast Exponentially Linear Unit (FELU) activation function to speed up the network running time. Lin et al [24] presented an improved unsaturated nonlinear segment activation function SignReLu, which alleviated the problem of gradient disappearance.

Although the above researches have obtained some achievements under specific conditions, they are carried out in

the case of weak noise. However, in actual production, the collected data often face strong noise interference, so it is very important to develop a model that can effectively solve the complexity caused by strong noise interference. In this paper, to solve problems of low accuracy and poor generalization performance of traditional models under strong noise conditions, a rolling bearing fault diagnosis method based on multi-scale pooling residual convolutional neural network (MSPRCNN) is proposed. The MSPRCNN model first realizes the extraction of feature information at different levels by combining the multi-scale pooling feature extraction module with the position upsampling module. Then, the gated convolution is used to further learn the extracted features with noise, and finally the Softmax classifier is adopted to complete the classification task of bearing faults. In addition, a new activation function IReLU is presented and applied to the MSPRCNN model to improve the fault recognition performance. The main contributions of this paper are summarized as follows:

1) Wide convolution kernel is used for feature extraction. The wide convolution kernel has a larger receptive field and can cover a wider range of input data, which can better capture the overall pattern and global correlation of the input data, avoid information loss, and improve the fault diagnosis performance of the overall model. By introducing a wide convolution operation, the MSPRCNN model has improvement in accuracy under the condition of SNR of −10dB~6dB.

2) A MSPFE module combined with UPA is proposed. The MSPFE module can extract features at different levels by pooling the input data at different scales. In this way, various details and features in the vibration signal can be captured more comprehensively, including different frequencies and amplitudes. By combining features of different scales, the multi-scale pooling feature extraction module can provide richer and more comprehensive information representation, thereby improving the performance of the MSPRCNN model.

3) Gated convolution and a new activation function IReLU are put forward. Gated convolution combined with IReLU activation function can effectively utilize the nonlinear characteristics of function and the feature selection and information transmission ability of gated convolution, so as to improve the network 's ability to characterize complex data. In addition, retaining the advantages of the ReLU function, the IReLU activation function introduces a new continuous function in the negative half axis to overcome the shortcomings of ReLU function, so as to better activate the feature information and improve the accuracy of bearing fault diagnosis.

2. Theoretical backgrounds

2.1. One-dimensional convolutional neural network

1D-CNN is a variant of CNN, which is used to process one-dimensional sequence data such as time series data and signal data. Different from 2D-CNN, 1D-CNN has unique advantages in processing time series data. 1D-CNN usually includes a convolutional layer, a pooling layer, an activation function layer, and a fully connected layer. The convolution layer extracts local features of the input sequence data through the convolution operation, which is similar to the feature extraction of the image in 2D-CNN.The pooling layer is adopted to reduce the length and number of feature sequences to decrease the complexity of the model. The activation function layer is used to activate each element. The fully connected layer maps the extracted features to the output category.

2.2. Pooling and unpooling

Pooling is a down-sampling operation to reduce the dimensions and parameters of data. It combines multiple adjacent data points into one output value by aggregating the local areas of the input data. The common pooling operations are Max Pooling and Average Pooling. The purpose of pooling is to preserve main features of input data, reduce the sensitivity to location information and the amount of data, improve computational efficiency and prevent overfitting. Global Average Pooling (GAP) is a special average pooling operation, which is robust to different sizes of input.

Unpooling or up-sampling is the inverse process of pooling operation, which is used to restore the down sampled data to the original size. Unpooling refills the lost information in the pooling operation by interpolation or replication.

Pooling and unpooling operations are often widely used in time series data, audio signal processing and models such as CNNs [25-26]. The advantages of pooling and unpooling operations in 1D-CNN are that they can effectively compress features, improve the robustness of the model, and recover lost details when needed, thereby improving the performance of

model.

2.3. Gated Convolution

Gated convolution is a convolutional neural network structure used to process sequential data. The basic idea is to introduce a gating mechanism to control the output of convolution operations. Gated convolution can adaptively select and retain the information in the input sequence through the gated information learned, so as to improve the expressive ability of model.

In gated convolution, the commonly used gated mechanism is Gated Linear Unit (GLU). GLU consists of two parts: a convolutional layer and a gated layer. The convolutional layer is responsible for extracting features, while the gated layer determines which features should be retained [27]. The specific process is shown in formula (1)~ (3).

$$Gating_{y,x} = \sum\sum W_g \cdot I \tag{1}$$

$$Feature_{y,x} = \sum\sum W_f \cdot I \tag{2}$$

$$Gating_{y,x} = \text{Sigmoid}(Gating_{y,x}) \otimes \varphi(\text{Feature}_{y,x}) \tag{3}$$

where, $\otimes$ is element-by-element multiplication, Sigmoid is the Sigmoid function, φ indicates activation function, W_g and W_f are two different convolution filters, and I is the feature input.

3. Fault diagnosis method based on MSPRCNN

The traditional fault diagnosis method has the problems of inaccurate diagnosis when dealing with complex operating conditions such as strong noise and variable working conditions. In this paper, the MSPRCNN model is proposed by improving multi-scale CNN to solve the problem that strong noise and variable working conditions affect the performance of the model. This section describes in detail the structures of key modules in the MSPRCNN methodology to demonstrate the design features and specific functions of each module.

3.1. Multi-scale pooling feature extraction module

Traditional multi-scale convolution structures increase computational complexity and cannot effectively reduce the feature dimension, and pooling operation loses location information during feature down sampling. In order to enhance the neural network's perception ability for features of different scales, extract feature representations with richer semantic information, and reduce the loss of location information, a multi-scale pooling feature extraction (MSPFE) module is proposed. The MSPFE module captures multi-scale feature information by pooling input data at different scales, so that the MSPRCNN model can better adapt to input data of different sizes and maintain robustness even the input size changes. At the same time, the position attention module for up-sampling learns different position feature representations to improve position variation robustness. The specific structure is shown in figure 1.

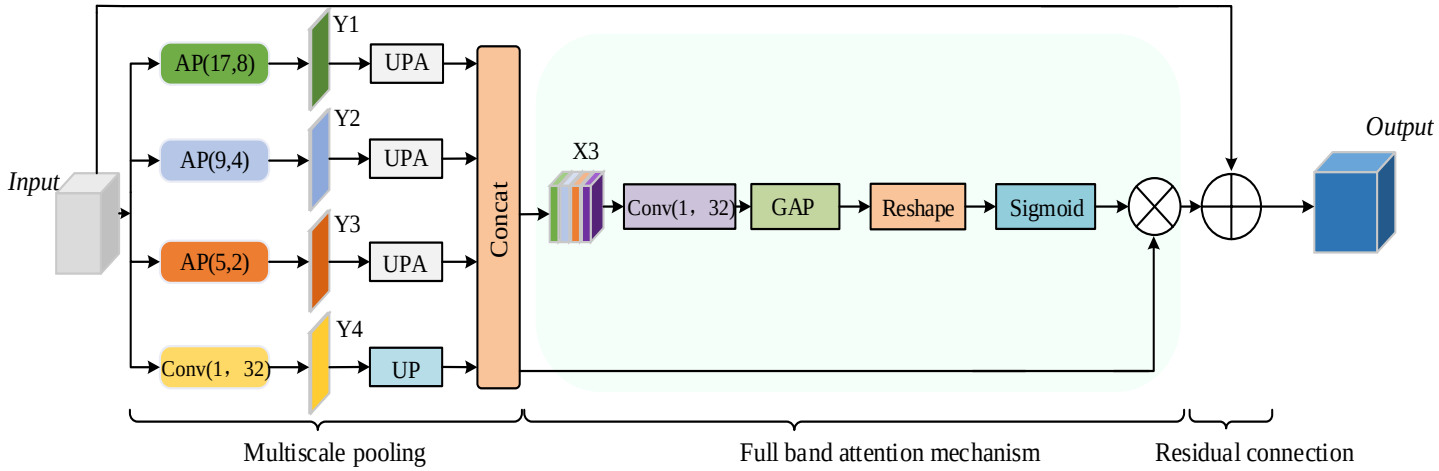

Figure 1. Multi-scale pooling feature extraction module.

The MSPFE module uses three different scales of pooling to provide relatively balanced feature representation, covering different levels of feature information. The MSPFE module selects three average pooling windows with 17, 9, and 5 pooling cores, which are relatively large and suitable for capturing a wider range of feature information. The pooling window of 17 can cover a longer feature sequence and capture global information. The pooling window of 9 and 5 can further refine

the feature representation and extract local features. Here, the steps of 8, 4 and 2 are selected to maintain a certain degree of overlap under different pooling windows to ensure the continuity and integrity of feature information. The MSPFE module performs feature extraction by using three average pooling windows and a point-by-point convolution with a channel number of 32 to form a multi-scale pooling operation to obtain features Y1, Y2, Y3, and Y4, respectively.

The average pooling reduces the data dimension and extracts the main features by defining the size of the pooling window and calculating the average value of the elements in the window. The specific process of average pooling operation is shown in formula (4).

$$y[i] = \frac{1}{k}\sum_{j=0}^{k-1} x[i \times k + j] \tag{4}$$

where, $y[i]$ is the output value after pooling, i is the output position, x is the input data, k is the size of the pooling window, and j is the index variable for iterative calculation.

The point-by-point convolution is introduced to adjust the number of output channels without increasing the computational complexity, and to transform the dimension of the feature tensor between the multi-scale feature layers. After the multi-scale pooling operation, the up-sampling position attention module is connected for up-sampling, which makes the model better recover the position information and maintain the scale invariance. The purpose of introducing up-sampling after point-by-point convolution operation is to improve the detail information and processing effect of the signal by increasing the number of sampling points, so as to complete the mutual fusion between features. After fusing features, this paper proposes a full-band attention mechanism to achieve the goal of attention mechanism allocation to guide fusion features. Point-by-point convolution compresses the channel of feature information, GAP provides global information for the receiving domain, Reshape changes the feature size, and Sigmoid function assigns weights to fusion features. In order to make the network adapt to complex data distribution and learning tasks, the MSPFE module introduces residual connection to stack the input features and the obtained features as output.

3.2 Up-sampling position attention module

In the multi-scale pooling operation, due to the down-sampling of feature information, some position information is lost. Therefore, an up-sampling position attention (UPA) module is introduced after each layer of pooling operation. The UPA module can recover the lost location information during the up-sampling process, and handle the positional relationship in the feature information, including the relative position and global positional relationships between the feature information, enabling the model to better reconstruct features and extract information of different scales. The UPA module structure is shown in figure 2.

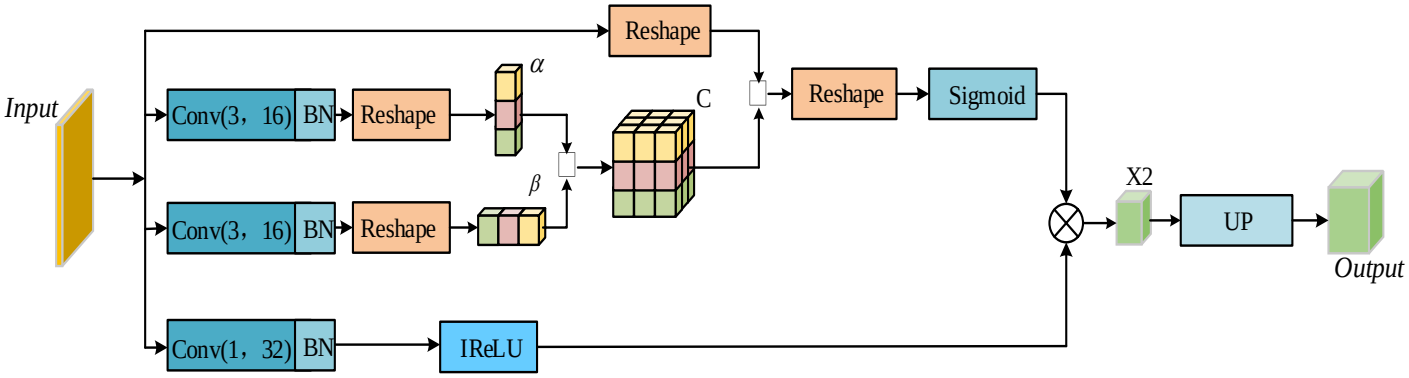

Figure 2. Up-sampling position attention module.

The UPA module introduces an outer product operation. The outer product operation is an important concept in linear algebra, which is used to multiply two vectors to generate a matrix, and represented by the symbol '⊙' in the figure 2. As can be seen from figure 2, the UPA module first converts the module extracted from the convolution with a convolution kernel size of 3 to α and β under two vectors through the Reshape operation, and generates the matrix C through the outer product operation. Then, the matrix C and the vector obtained by the input feature reconstruction are subjected to an outer product operation to generate a higher-dimensional tensor, and then it is converted into a vector by the Reshape operation. Two outer

product operations can not only introduce more feature interaction information between different dimensions, to capture the complex patterns and relationships in the input data, but also introduce more high-order feature interaction information to improve the nonlinear expression ability of the model. Finally, the channel number of input feature is changed by point-by-point convolution, and then the feature X2 is obtained by multiplying the elements with the features processed by the Sigmoid function. Subsequently, the feature X2 is up-sampled to obtain the output feature. After each layer of convolution, the Batch Normalization (BN)regularization operation is added to avoid over-fitting of the model during training. The specific process is shown in formula (5)~ (6).

$$Y = Re\,\mathrm{shape}A_l \otimes (Re\,\mathrm{shape}A_q \otimes Re\,\mathrm{shape}A_k) \quad (5)$$

$$Output = \mathrm{Up}[\mathrm{Sigmoid}(Re\,\mathrm{shape}Y) \otimes A_v] \quad (6)$$

where, A_l is the module input feature, $A_q$and A_k are the features obtained by convolution normalization, A_v is the feature after convolution, normalization and IReLU function activation, Up is up-sampling operation, Reshape is the operation of changing the shape of the input data, and Y is the high-dimensional tensor obtained by the outer product operation.

3.3. Gated convolution

In order to utilize the information of different positions in the sequence, reduce the over-fitting of model, and improve the identification accuracy and generalization ability of network, the Gated Convolution (GC) is introduced, and its structure is shown in figure 3.

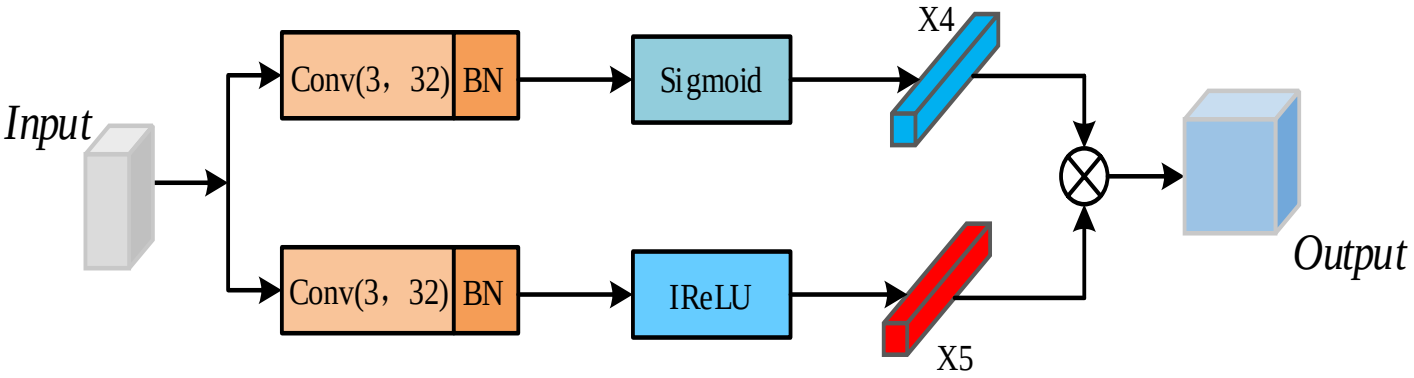

Figure 3. Gated convolution.

GC introduces a gating unit to control the transmission and screening of features, which improves the modeling ability of model for long-distance dependence. Firstly, the input features in the GC module are decomposed into two parts. The convolution with a convolution kernel size of 3 is used to capture the local features in the input sequence. In addition, the normalized layer BN is added after the convolution, which can accelerate the model training and alleviate the problem of gradient disappearance. Secondly, the Sigmoid function is used to control the transmission of information, so as to obtain the feature X4, and the IReLU function is used to control the neglect of information, so as to obtain the feature X5. Finally, the feature X4 and X5 are fused by element multiplication to obtain the output. This mechanism allows the network to selectively learn the interaction between features, thereby improving the performance of network. The specific process is shown in formula (7).

$$X = \mathrm{Sigmiod}\ (W \cdot x_i + b)\ \otimes \mathrm{IReLU}\ (W' \cdot x_i + b') \quad (7)$$

where, x_i is the ith element in the input sequence, W and W' are convolution filters, b and b' are bias values, IReLU is the IReLU activation function, and X is the output of gated convolution operation.

3.4. Activation function-IReLU

After extracting features, in order to enhance the nonlinear expression ability of model, it is necessary to use the activation function to activate the features. In neural network-based models, common activation functions include ReLU, Tanh and ELU. However, the traditional function has some problems. For example, the ReLU function will directly set the negative value to zero, which leads to the loss of important information. Tanh and ELU have the problem of gradient disappearance. In order to solve these problems, a new activation function IReLU is proposed, and the function image is shown in figure 4. The calculation formula of IReLU is shown in Equation (8).

$$f(x) = \begin{cases} x & (x > 0) \\ \frac{e^x - 1}{e^x + 1} & (x \leq 0) \end{cases} \quad (8)$$

The derivative function of $f(x)$ is shown in equation (9).

$$f'(x) = \begin{cases} 1 & (x > 0) \\ \frac{2e^x}{(e^x + 1)^2} & (x \leq 0) \end{cases} \quad (9)$$

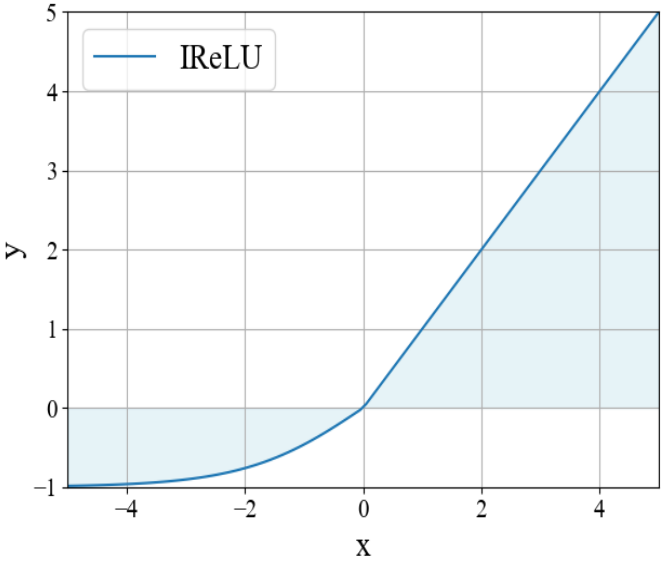

Figure 4. IReLU activation function.

It can be seen from equation (9) that when $x = 0$, $f'(x) = \frac{1}{2}$, when $x < 0$, $f'(x) > 0$. The derivative of IReLU is always in the (0, 1) interval on the negative half axis, which avoids the saturation problem of Tanh and ELU activation functions in the negative region. The derivative of value on positive half axis is always 1, which means that the gradient will not disappear in the positive input range, which is conducive to the transmission of information and the update of gradient. Different from ReLU and ELU where the derivative value is 0 at point 0, the IReLU function has a clear derivative value when the input is 0, which improves the convergence speed of the network and reduces the training time. At the same time, the participation of negative input signals introduces some control noise into the network, which alleviates the mandatory sparsity of activation function. Therefore, it shows that the IReLU activation function can better support the training and optimization of deep learning model, and can better cope with the problems such as gradient vanishing and exploding, thus improving the training effect of model.

3.5. Fault diagnosis process based on MSPRCNN

In the MSPRCNN model, the original vibration signal is first converted into a frequency domain signal using Fourier Transform as the input of MSPRCNN method. Then, a wide convolution kernel is used to extract features, and a multi-scale pooling feature extraction module combined with the Up-sampling position attention mechanism is introduced to adaptively extract features of different scales. Next, the feature representations of different scales are stacked together on the channel dimension through the Concat operation. Among them, the multi-scale pooling operation performs feature extraction at different scales, which resists the interference of strong noise and improves the robustness of model, and enables the network to adapt to different operating conditions. The Up-sampling position attention module promotes the MSPFE module to better understand the importance and relevance of different positions in the sequence data, thereby extracting more representative and discriminative feature information, and improving the accuracy and reliability of model in time series prediction and analysis tasks. Through feature fusion, information at different scales can be retained, which enables the network to better understand data features and distinguish effective features from noise, thereby improving accuracy and robustness.

Secondly, ordinary convolution and gated convolution are used to further extract and learn the features with noise. The structure of gated convolution enables the network to adaptively select the appropriate receptive field to extract key information. Then, in order to prevent gradient disappearance and explosion, residual connection is introduced, and the features extracted by the first layer convolution are fused with the features processed by gated convolution. In the next diagnostic process, the maximum pooling and global average pooling are used successively to further reduce the data dimension while retaining important features. In addition, inserting the Group Normalization (GN), MSPFE module and UPA module, can better adapt to the data distribution at different scales and reduce computational complexity. Finally, the fusion features are identified and classified through the fully connected layer and the Softmax layer. The structure of MSPRCNN is shown in figure 5. The details of model constructed in this paper are shown in table 1. The number of neurons in the fully connected layer is 100, and the number of neurons in the Softmax layer is 7.

4. Experimental validation

4.1. Rolling bearing data set construction

In this paper, the bearing data set of Case Western Reserve University (CWRU) and the data set collected by the MFS fault simulation test bench of our laboratory are used for experimental verification. The sample length of both data sets is set to 2048. In the anti-noise experiment, the randomly generated Gaussian white noise is added to the original signal, and the size of SNR is adjusted to simulate the influence of different degrees of noise.

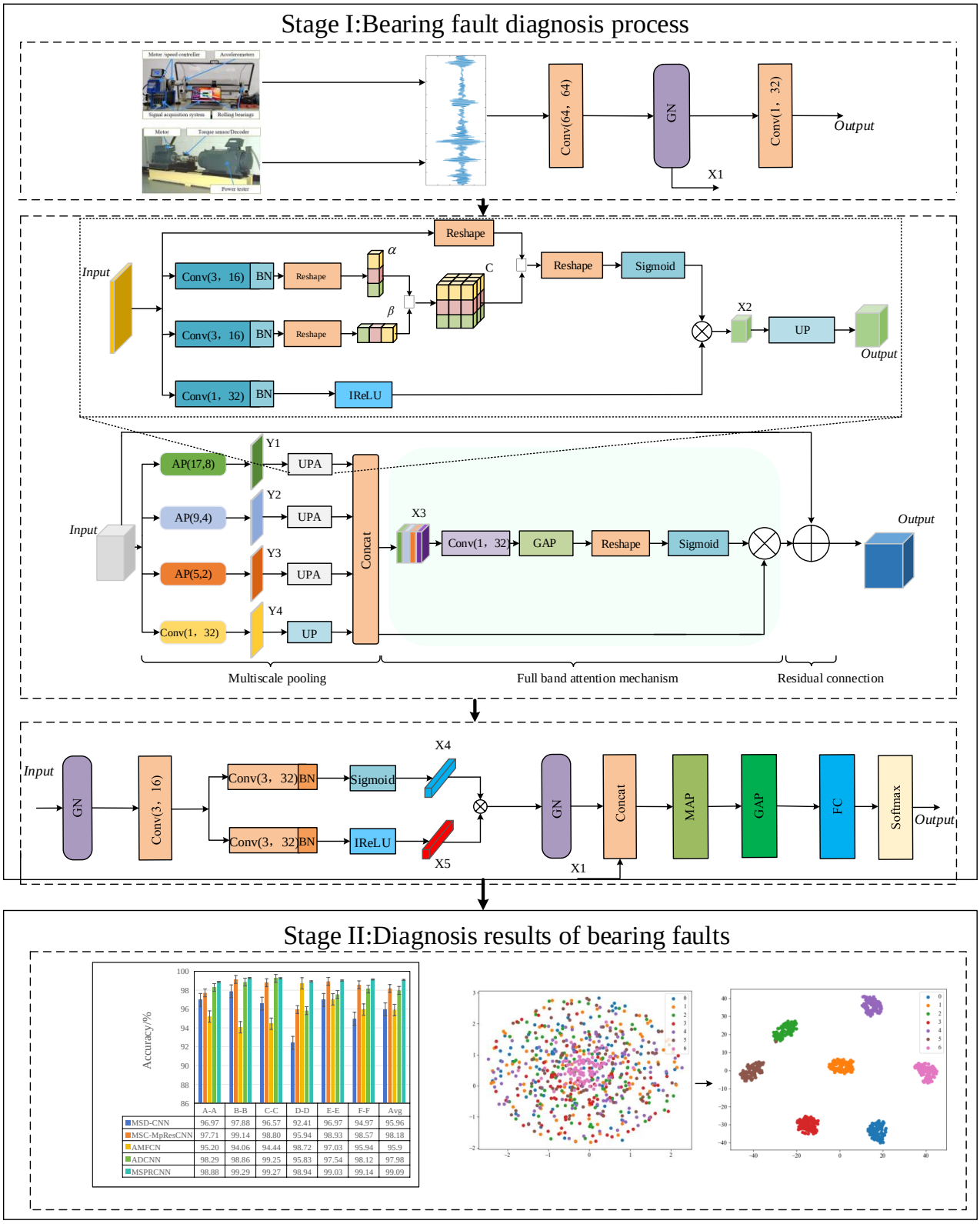

	A-A	B-B	C-C	D-D	E-E	F-F	Avg
MSD-CNN	96.97	97.88	96.57	92.41	96.97	94.97	95.96
MSC-MpResCNN	97.71	99.14	98.80	95.94	98.93	98.57	98.18
AMFCN	95.20	94.06	94.44	98.72	97.03	95.94	95.9
ADCNN	98.29	98.86	99.25	95.83	97.54	98.12	97.98
MSPRCNN	98.88	99.29	99.27	98.94	99.03	99.14	99.09

Figure 5. MSPRCNN model.

Table 1. MSPRCNN optimal structure parameters.

Layer Type	Convolutional kernel size	Number of convolutional kernels	Output size
Input	/	/	2048×1
Conv1D_1	7	64	2048×64
Group Normalization 1	/	/	2048×64
Conv1D_2	1	32	2048×32
MSPFE	/	/	2048×32
Group Normalization 2	/	/	2048×32
Conv1D_3	3	16	2048×16
GC	/	/	2048×32
Group Normalization 3	/	/	2048×32
Concatenate	/	/	2048×96
Max Pooling	/	/	1024×96
Global Average Pooling	/	/	1×96
Fully connected	/	100	100
Dropout	/	/	100
Softmax	/	7	7

Data set 1 is the CWRU rolling bearing data set [28], and the CWRU bearing fault test bench is shown in figure 6 (a). The bearing model is SKF6205, the sampling frequency is 12kHz, and the load is 1hp␣ 3hp. The failure mode is pitting corrosion, the diameters are 0.18 mm and 0.36 mm, respectively, and the single point failure is formed by EDM. There are 7 fault types, including inner ring, outer ring, and rolling element fault and normal state. The data sets are denoted as A, B and C, corresponding to loads of 1hp, 2hp and 3hp, respectively. The operating conditions and fault information of CWRU are shown in table 2.

Data set 2 is the MFS bearing data set of our laboratory, and the MFS fault diagnosis test bench is shown in figure 6 (b). The bearing model is ER-16K, and the faults are inner ring fault, outer ring fault and rolling element fault, as shown in figure 7. The sampling frequency is 15.36kHz, and the rotation speeds are 1200rad/min, 1300rad/min and 1400rad/min, respectively. The corresponding data sets are recorded as D, E and F, respectively. The fault is processed by laser etching technology, with a diameter of 0.6mm and 1.2mm, a total of 7 fault types. The operating conditions and fault information of MFS are shown in table 3.

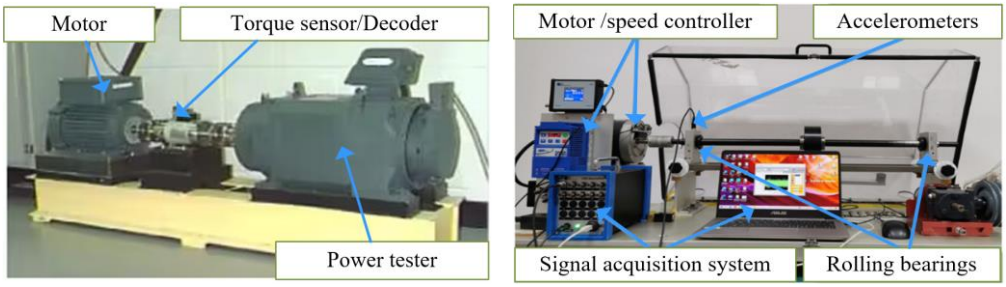

(a)CWRU mechanical fault simulation test platform (b)MFS mechanical fault simulation test platform

Figure 6. Test platform.

Table 2. CWRU rolling bearing data set.

Fault diameter /mm		0	0.18			0.36			Load
		Normal	Inner ring	Outer ring	Rolling element	Inner ring	Outer ring	Rolling element	
	Label	0	1	2	3	4	5	6	
A	Training set	100	100	100	100	100	100	100	1hp
	Testing set	100	100	100	100	100	100	100	(0.7457kW)
B	Training set	100	100	100	100	100	100	100	2hp
	Testing set	100	100	100	100	100	100	100	(1.4914kW)
C	Training set	100	100	100	100	100	100	100	3hp
	Testing set	100	100	100	100	100	100	100	(2.2371kW)

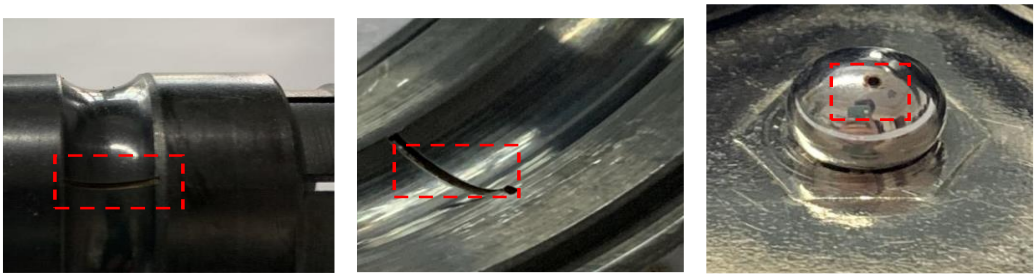

(a) Inner ring fault (b) Outer ring fault (c) Rolling element fault

Figure 7. Fault location of rolling bearing.

Table 3. MFS rolling bearing dataset.

Fault diameter /mm		0	0.6			1.2			Revolution speed
		Normal	Inner ring	Outer ring	Rolling element	Inner ring	Outer ring	Rolling element	
	Label	0	1	2	3	4	5	6	
D	Training set	100	100	100	100	100	100	100	1200 $rad \cdot min^{-1}$
	Testing set	100	100	100	100	100	100	100	
E	Training set	100	100	100	100	100	100	100	1300 $rad \cdot min^{-1}$
	Testing set	100	100	100	100	100	100	100	
F	Training set	100	100	100	100	100	100	100	1400 $rad \cdot min^{-1}$
	Testing set	100	100	100	100	100	100	100	

Figure 8 shows the comparison between the frequency domain signal of original signal after Fourier transform and the frequency domain signal after adding Gaussian white noise. From the figure 8, the characteristics of the original signal and the change of the frequency domain spectrum with Gaussian white noise can be clearly observed.

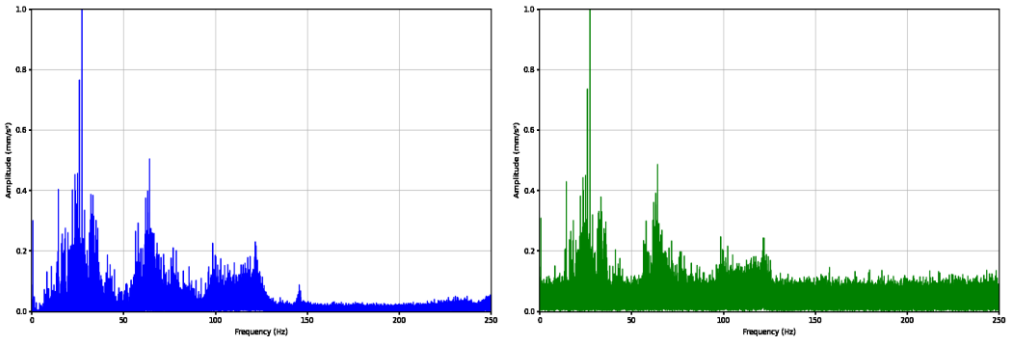

(a) Original signal (b) −4dB

Figure 8. Frequency domain diagram.

4.2. Selection of parameters

In the experiment of this paper, the software version is PyCharm2020.1.2. The software environment is Tensorflow, and the hardware configuration is Intel (R)Xeon-(R)Silver 4110 CPU, 64-GB RAM, NVIDIA Quadro P4000 GPU. The experimental optimizer uses Adam optimizer, and the number of training is 30 times. In order to reduce the error, all experiments are tested 10 times and averaged.

The selection of hyperparameters is very important to improve the diagnostic performance of model. Therefore, the parameter selection experiments are carried out under the conditions of A-B and A-C and SNR of-6dB, –4dB and –2dB, respectively. Among them, A-B means that the training set adopts data set A, and the test set adopts data set B. The experimental results are shown in figures 9 and 10. Because the width of first layer convolution kernel has a great influence on the performance of model, wide convolutions with kernel sizes of 16, 32, 64, 128 and 256 are tried for comparison experiments. It can be seen from figure 9 (a) and figure 10 (a) that when the

convolution kernel width is 64, the performance of model is optimal. Therefore, the convolution layer with a kernel width of 64 is selected. In addition, the appropriate batch size and learning rate are also very important for model performance. It is observed from figures 9 and 10 that when the batch size is 8 and the learning rate is 0.0005, the model performance is optimal. These choices can effectively control the computational complexity and parameters while improving model performance.

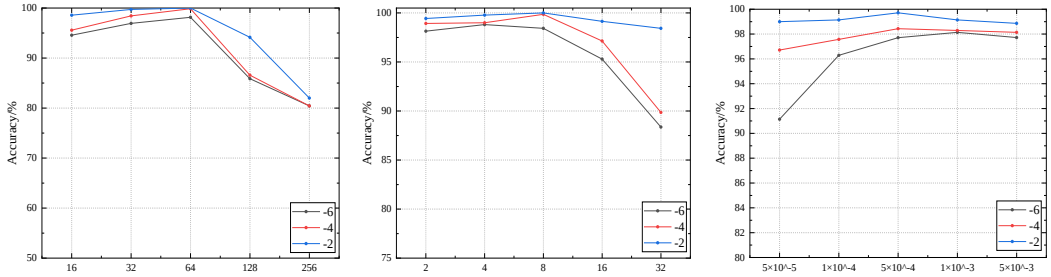

(a) Wide convolution kernel selection (b) Batch size selection (c) Selection of learning rate

Figure 9. Hyperparamete selection under A-B condition.

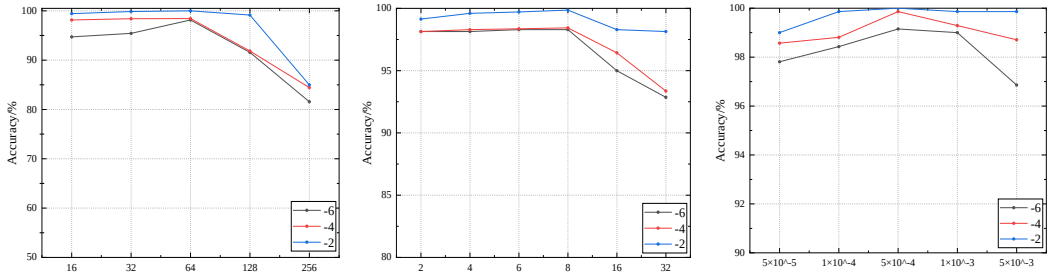

(a) Wide convolution kernel selection (b) Batch size selection (c) Selection of learning rate

Figure 10. Hyperparamete selection under A-C condition.

4.3. Validation

In order to verify the effectiveness of proposed method, this model is compared with MSD-CNN [29], MSC-MpResCNN [30], AMFCN [31], ADCNN [32] models under the condition of SNR= −4dB. Among them, MSD-CNN is a multi-scale deep convolutional neural network, and MSC-MpResCNN is a multi-scale cascaded midpoint residual convolutional neural network. AMFCN is an adaptive multi-scale fully convolutional network that uses large kernel convolution for feature extraction. ADCNN is an adaptive denoising convolutional neural network.

The fault diagnosis results of above methods under the same working conditions are shown in figure 11. It can be seen from figure 11 that the above methods show good fault recognition performance under noise conditions, but the classification accuracy of this method is higher, and the recognition accuracy under all working conditions is more than 98%. At the same time, the average accuracy of MSPRCNN model reaches 99.09%, which is 0.91% higher than that of MSC-MpResCNN, 1.11% higher than that of ADCNN, 3.13% higher than that of MSD-CNN, and 3.19% higher than that of AMFCN. These results clearly show that the proposed method can realize fault identification in noisy environment, and has higher fault classification performance than other methods.

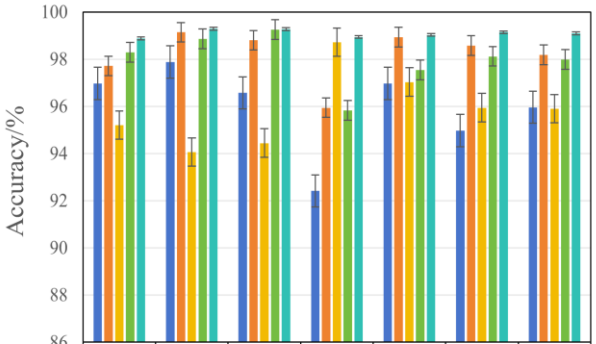

	A-A	B-B	C-C	D-D	E-E	F-F	Avg
MSD-CNN	96.97	97.88	96.57	92.41	96.97	94.97	95.96
MSC-MpResCNN	97.71	99.14	98.80	95.94	98.93	98.57	98.18
AMFCN	95.20	94.06	94.44	98.72	97.03	95.94	95.9
ADCNN	98.29	98.86	99.25	95.83	97.54	98.12	97.98
MSPRCNN	98.88	99.29	99.27	98.94	99.03	99.14	99.09

Figure 11. Fault diagnosis results under the same working conditions.

4.4. Experimental verification under variable conditions

In actual production, the operating conditions of mechanical

equipment are often complex and changeable situations, among which variable load and variable speed are the most common situations. Under the influence of these factors, it is very important to diagnose the fault information stably. In order to verify the generalization ability of MSPRCNN model under different working conditions, the fault diagnosis results of MSPRCNN and other models are compared and analyzed under SNR = −4dB and variable working conditions.

4.4.1. Experimental analysis under variable load

The classification results of MSPRCNN model and other methods under variable load are shown in figure 12, where A-B represents the data set A as the training set and B as the test set.

It can be observed from figure 12 that the average accuracy of proposed method reaches 98.71%, which is 1.33%␣ 6.25% higher than other methods. Under six working conditions, the fault diagnosis accuracy of MSPRCNN method is the highest under working conditions A-B, reaching 99.86%, which is 6.6% higher than that of AMFCN with the lowest diagnostic accuracy and 0.83% higher than that of ADCNN with the highest diagnostic accuracy. The lowest accuracy under the working condition B-A is 98.34%, which is 0.63% higher than the ADCNN.

At the same time, the error line in the figure 12 shows that the stability of proposed method is also significantly higher than other methods. Therefore, it can be concluded that the MSPRCNN model has excellent fault recognition performance and generalization ability under strong noise and variable load conditions.

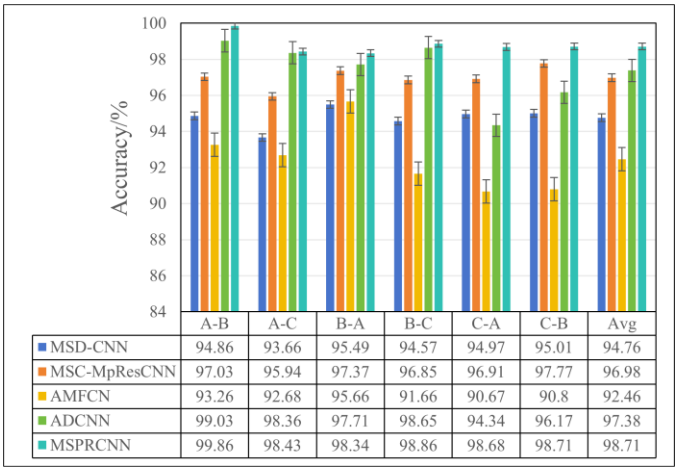

	A-B	A-C	B-A	B-C	C-A	C-B	Avg
MSD-CNN	94.86	93.66	95.49	94.57	94.97	95.01	94.76
MSC-MpResCNN	97.03	95.94	97.37	96.85	96.91	97.77	96.98
AMFCN	93.26	92.68	95.66	91.66	90.67	90.8	92.46
ADCNN	99.03	98.36	97.71	98.65	94.34	96.17	97.38
MSPRCNN	99.86	98.43	98.34	98.86	98.68	98.71	98.71

Figure 12. Fault diagnosis results under variable load.

In order to observe the misclassification of faults more clearly, a confusion matrix is used for visual comparative analysis in operating conditions A-B. At the same time, the diagnostic performance of MSPRCNN model is analyzed by controlling the SNR in condition A-C. The diagnosis results are shown in figure 13 and 14, respectively.

It can be seen from figure 13 that in strong noise environment with SNR = −4dB, the MSPRCNN can accurately identify most faults, but there are also some fault categories that are misclassified. Among the 100 samples of 0.18mm outer race faults, 3 samples are misdiagnosed as 0.36mm rolling element faults, resulting in a misdiagnosis rate of 3%. ADCNN, which has the highest classification accuracy among other comparison methods, misclassified 0.36mm rolling element faults as 0.18mm inner ring faults, leading to misdiagnosis rate of 12%. This further validates the diagnostic advantages of proposed method in the diagnosis of rolling bearing faults.

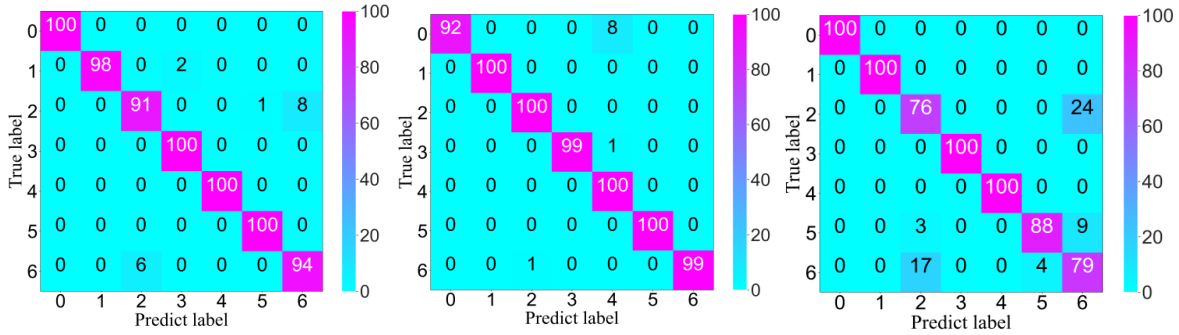

(a) MSD-CNN (b) MSC-MpResCNN (c) AMFCN

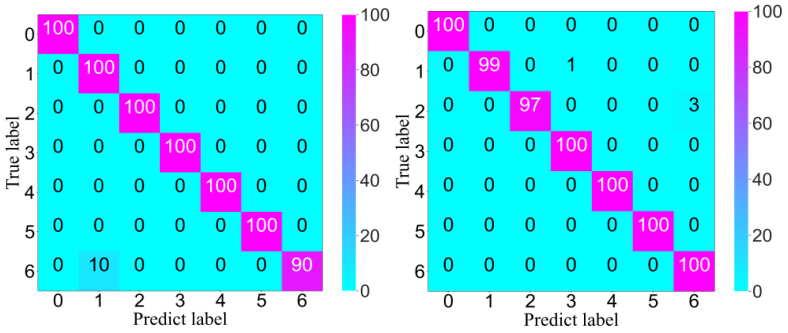

(d) ADCNN (e) MSPRCNN

Figure 13. Confusion matrix under variable load.

It can be seen from figure 14 that the diagnostic performance of MSPRCNN model improves with the increase of SNR. When SNR = −10dB, 79 out of 700 test samples are misclassified, and when SNR = −4dB, only 8 samples are misclassified. This indicates that the MSPRCNN model also has better diagnostic performance at higher SNRs. By analyzing the confusion matrix, the performance of system under different working conditions can be evaluated more clearly, which provides a useful reference for further optimizing the algorithm. Overall, the MSPRCNN model has higher fault recognition performance in strong noise environment.

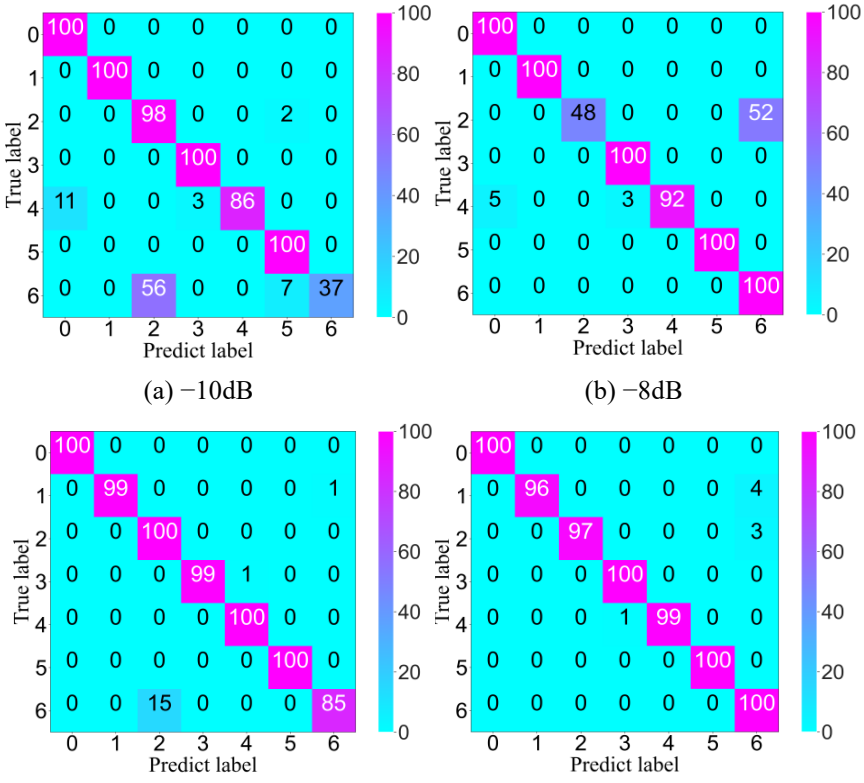

(a) −10dB (b) −8dB

(c) −6dB (d) −4dB

Figure 14. Confusion matrix under different SNRs.

4.4.2. Experimental analysis under variable speed

The MSPRCNN model is compared with the other four comparison methods under variable speed conditions, and the experimental results are shown in figure 15. It can be seen that the average recognition accuracy of MSPRCNN model reaches 98.2 %, which is 1.51 % higher than that of MSC-MpResCNN with the highest accuracy among four comparison methods, and 4.38 % higher than MSD-CNN with the lowest accuracy. This shows that the MSPRCNN model has stronger anti-interference ability in noisy environment. In the working condition E-F, the accuracy of model proposed reaches 99.14%, which is 1.37% higher than that of the best AMFCN accuracy. This shows that the MSPRCNN method has stronger feature recognition effect,

more accurate extraction of useful features in noisy environment, and improves the accuracy of fault diagnosis. At the same time, by observing the error line in the graph, it can be found that the recognition stability of MSPRCNN model is better than other methods when SNR = −4, which proves that the proposed method has stronger stability performance. In summary, these results show that the MSPRCNN model has better performance under variable speed conditions.

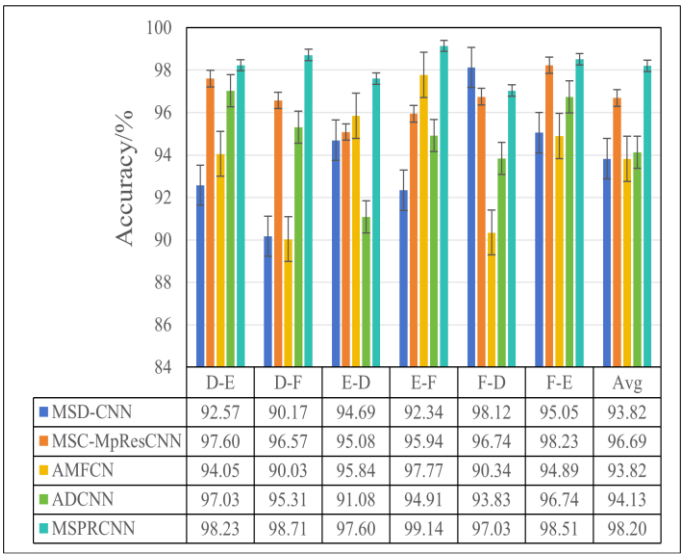

	D-E	D-F	E-D	E-F	F-D	F-E	Avg
MSD-CNN	92.57	90.17	94.69	92.34	98.12	95.05	93.82
MSC-MpResCNN	97.60	96.57	95.08	95.94	96.74	98.23	96.69
AMFCN	94.05	90.03	95.84	97.77	90.34	94.89	93.82
ADCNN	97.03	95.31	91.08	94.91	93.83	96.74	94.13
MSPRCNN	98.23	98.71	97.60	99.14	97.03	98.51	98.20

Figure 15. Fault diagnosis results under variable speed.

In order to further prove the performance of this method under stronger noise conditions, different SNRs are selected for experimental comparison under working conditions D-F. As shown in figure 16, the fault accuracy of above methods in different noise environments is shown. It can be seen from figure 16 that the stronger the noise, the more obvious the diagnostic performance advantage of MSPRCNN model. When the SNR is −10 dB, the fault accuracy of MSPRCNN reaches 86.57%, which is 4.34% higher than AMFCN, 9.05% higher than MSC-MpResCNN, 14.93% higher than MSD-CNN, and 16.38% higher than ADCNN. With the increase of SNR, the accuracy of above methods increases, while the change range of method proposed is the smallest, which shows that the MSPRCNN model is less sensitive to noise. When the SNR = 4dB, the accuracy of MSPRCNN model reaches 100%, which is 0.29%␣ 0.57% higher than other models. In summary, under the condition of strong noise, the MSPRCNN model can effectively suppress noise interference, improve the accuracy and stability of fault identification, and provide reliable technical support for monitoring the operation status of industrial equipment.

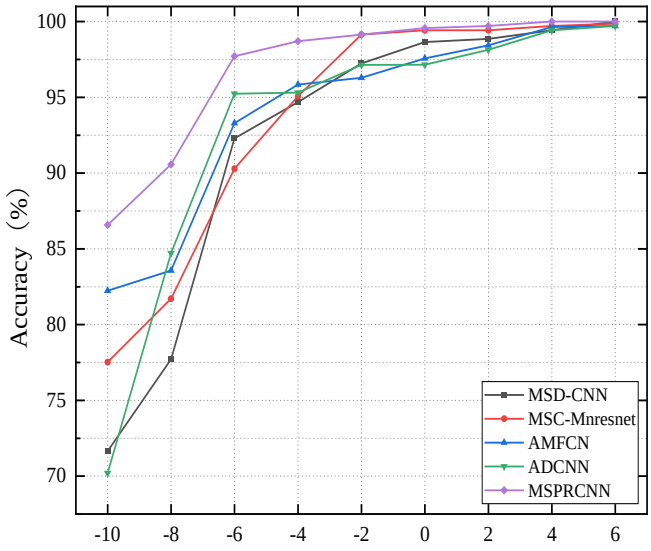

Figure 16. Fault diagnosis results under different signal-to-noise ratios.

In order to further evaluate the effectiveness of MSPRCNN model in fault identification, t-distributed stochastic neighborhood embedding (t-SNE) is used to visualize the distribution of features under the condition of SNR = −4dB. The fault classification results are shown in figure 17. It can be seen that the feature information learned by the MSPRCNN model exhibits good discriminative ability for various fault types. Within the same fault category, features have better clustering performance, while features from different fault categories are easier to separate, which indicates that the MSPRCNN model can effectively distinguish different types of faults and cluster the same type of fault features.

4.4.3. Experimental analysis under mixed load conditions

In order to test the diagnostic performance of proposed diagnostic method under mixed load conditions, comparative experiments under variable load mixed conditions are conducted. Among them, A+B represents the fusion of data under condition A and condition B, A+B-C represents A + B as the training set and C as the test set. The experimental results are shown in figure 18. It can be clearly seen that the MSPRCNN model has higher prediction accuracy than other diagnostic methods under three different mixed conditions.

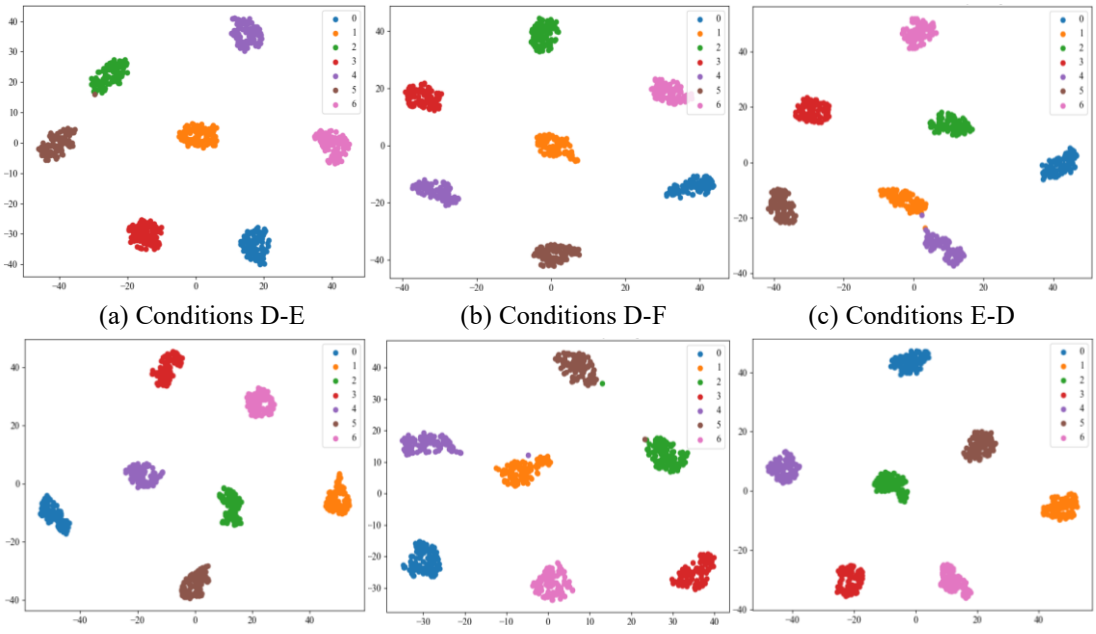

(a) Conditions D-E (b) Conditions D-F (c) Conditions E-D

(d) Conditions E-F (e) Conditions F-D (f) Conditions F-E

Figure 17. Visualization of t-SNE under variable speed.

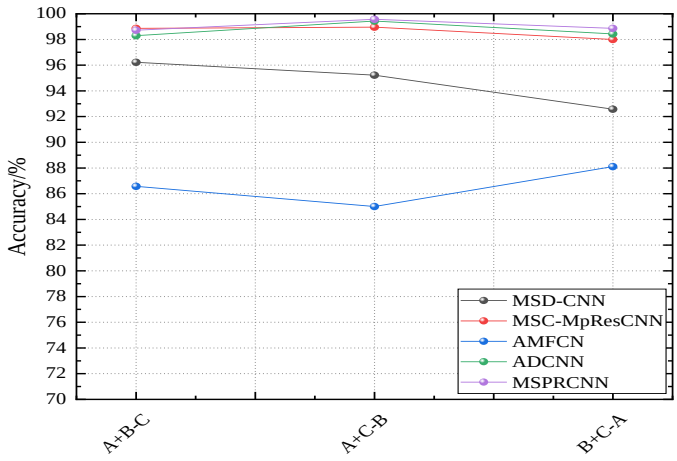

Figure 18. Experimental comparison of variable load mixed conditions.

4.5. Ablation experiment

In this section, ablation experiments are carried out under A-B conditions to verify the role of each module presented in this paper. The comparative models designed are as follows. MSPRCNN1 is the MSPRCNN model without the wide convolutional layer. MSPRCNN2 is the MSPRCNN model without the MSPFE module. MSPRCNN3 is the MSPRCNN model without the GC module. MSPRCNN4 is the MSPRCNN model with ReLU activation function instead of IReLU function.

The experimental results are shown in table 4. The diagnostic accuracy of MSPRCNN1 model is significantly reduced. When SNR = −4dB, the fault recognition accuracy is reduced from 99.86% to 79.29%, which shows that the wide convolution module plays a key role in feature extraction and pattern recognition. The accuracy of MSPRCNN2 model is lower than that of the MSPRCNN model. When SNR = −10, the accuracy rate is 87.43%, which is 2.43% lower than that of MSPRCNN, which indicates that the MSPFE module plays an important role in improving the attention and discrimination ability of the model to key features. The accuracy of MSPRCNN3 model is also lower than that of MSPRCNN method, which shows that the GC module plays an important role in the connection and information transmission of model. The diagnostic performance of MSPRCNN4 model is also lower than that of MSPRCNN. When SNR = −10 dB, the accuracy rate reaches 85.43%, which is 4.43% lower than that of MSPRCNN method, which exhibits that the introduction of nonlinear IReLU activation function will alleviate the gradient disappearance of model and improve the expression ability and generalization ability of model.

Based on the above results, it is concluded that each module has an important impact on the overall model performance. These analysis results provide important references for further optimizing the model, which is helpful to understand the relationship between model structure and performance, so as to design more efficient and accurate models.

Table 4. Ablation experimental results.

	SNR(dB)	−10	−8	−6	−4	−2	0	2	4	6
Accuracy(%)	IMSPRCNN1	77.57	78.64	78.86	79.29	86.14	88.03	90.71	94.43	97.29
	IMSPRCNN2	87.43	91.64	93.93	98.57	99.11	99.46	100	100	100
	IMSPRCNN3	88.57	90.86	93.14	98.43	98.86	99.43	99.14	99.29	100
	IMSPRCNN4	85.43	90.29	93.57	97.29	97.56	98.57	99.86	100	100
	MSPRCNN	89.86	91.79	94.52	98.86	98.95	99.82	100	100	100

5. Conclusion

Aiming at the influence of strong noise and variable working condition on the diagnostic performance of model, this paper proposes a fault diagnosis method based on MSPRCNN. In this method, the multi-scale pooling, up-sampling position attention, gated convolution and IReLU activation function are combined into the CNN. This structural design not only improves the ability of model to extract data features, but also enhances the robustness and generalization ability of network in dealing with complex problems. The following are the specific conclusions:

1) The wide convolution kernel is used for feature extraction. Global features in the vibration signal can be better captured by the wide convolution kernel. In addition, the wide convolution kernel provides a wider receptive field, which helps to increase the context information of signal. In the experiment, when the SNR is −4dB, the accuracy of MSPRCNN method is improved by 20.57% using the wide convolution kernel.

2) The MSPFE module is constructed. The MSPFE module combined with UPA can abstract and extract features at different levels, and understand the information in the vibration signal more comprehensively. In the verification experiment, when the SNR = −10 dB, the application of MSPFE module improves the diagnostic accuracy of MSPRCNN method by 2.43%.

3) The MSPRCNN model is proposed and the IReLU activation function is designed. The MSPRCNN model combines multi-scale pooling with gated convolution operations to effectively capture features at different time scales. The presented IReLU activation function enhances the nonlinear modeling ability of network. In the experiment, when SNR = −4dB, the accuracy of MSPRCNN model combined with IReLU activation function is 2.57 % higher than that of method without IReLU activation function.

4) The experimental results show that the MSPRCNN method shows better classification accuracy and stronger robustness in noisy environment. Specifically, the experimental results show that the average accuracy of variable load and variable speed of MSPRCNN model in noise environment reaches 98.71% and 98.2% respectively, which verifies the effectiveness and superiority of this method in dealing with strong noise interference and adapting to different working conditions.

Reference

1. He M, He D. Deep learning based approach for bearing fault diagnosis[J]. IEEE Transactions on Industry Applications, 2017, 53(3): 3057-3065. DOI: 10.1109/tia.2017.2661250
2. Sun HM, He DQ, Lao ZP, Jin ZZ, Liu C, Shan S. Fault diagnosis of train traction motor bearing based on improved deep residual network[J]. Proceedings of the Institution of Mechanical Engineers, Part C: Journal of Mechanical Engineering Science, 2024, 238(7): 3084-3099. DOI: 10.1177/09544062231196938
3. Du SC, Liu T, Huang DL, Li GL. An optimal ensemble empirical mode decomposition method for vibration signal decomposition[J]. Journal of Vibration and Acoustics, 2017, 139(3): 031003. DOI: 10.1115/1.4035480
4. Wang FT, Deng G, Liu CX, Su WS, Han QK, Li HK. A deep feature extraction method for bearing fault diagnosis based on empirical mode decomposition and kernel function[J]. Advances in Mechanical Engineering, 2018, 10(9): 1687814018798251. DOI: 10.1177/1687814018798251
5. He KM, Zhang XY, Ren SQ, Sun J. Spatial pyramid pooling in deep convolutional networks for visual recognition[J]. IEEE Transactions on Pattern Analysis and Machine Intelligence, 2015, 37(9): 1904-1916. DOI: 10.1109/tpami.2015.2389824
6. Krizhevsky A, Sutskever I, Hinton GE. ImageNet classification with deep convolutional neural networks[J]. Communications of the ACM, 2017, 60(6): 84-90. DOI: 10.1145/3065386
7. Zhao J, Yang SP, Li Q, Liu YQ, Gu XH, Liu WP. A new bearing fault diagnosis method based on signal-to-image mapping and convolutional neural network[J]. Measurement, 2021, 176: 109088. DOI: 10.1016/j.measurement.2021.109088
8. Wu GG, Ji XR, Yang GL, Jia Y, Cao CC. Signal-to-Image: Rolling bearing fault diagnosis using ResNet family deep-learning models[J].

Processes, 2023, 11(5): 1527. DOI: 10.3390/pr11051527

9. Zhang YH, Shang L, Gao HB, He YL, Xu XB, Chen YJ. A new method for diagnosing motor bearing faults based on gramian angular field image coding and improved CNN-ELM [J]. IEEE Access, 2023, 11: 11337-11349. DOI: 10.1109/access.2023.3241367
10. Xie SL, Ren GY, Zhu JJ. Application of a new one-dimensional deep convolutional neural network for intelligent fault diagnosis of rolling bearings[J]. Science Progress, 2020, 103(3): 0036850420951394. DOI: 10.1177/0036850420951394
11. Hakim M, Omran AAB, Inayat-Hussain JI, Ahmed AN, Abdellatef H, Abdellatif A, Gheni HM. Bearing fault diagnosis using lightweight and robust one-dimensional convolution neural network in the frequency domain[J]. Sensors, 2022, 22(15): 5793. DOI: 10.3390/s22155793
12. Chen XH, Zhang BK, Gao D. Bearing fault diagnosis base on multi-scale CNN and LSTM model[J]. Journal of Intelligent Manufacturing, 2021, 32(4): 971-987. DOI: 10.1007/s10845-020-01600-2
13. Chen JB, Huang RY, Zhao K, Wang W, Liu LC, Li WH. Multiscale convolutional neural network with feature alignment for bearing fault diagnosis[J]. IEEE Transactions on Instrumentation and Measurement, 2021, 70: 1-10. DOI: 10.1109/tim.2021.3077673
14. Zhao WL, Wang ZJ, Cai WA, Zhang QQ, Wang JY, Du WH, Yang NN, He XX. Multiscale inverted residual convolutional neural network for intelligent diagnosis of bearings under variable load condition[J]. Measurement, 2022, 188: 110511. DOI: 10.1016/j.measurement.2021.110511
15. Lee CY, Zhuo GL. Identifying bearing faults using multiscale residual attention and multichannel neural network[J]. IEEE Access, 2023, 11: 26953-26963. DOI: 10.1109/access.2023.3257101
16. Kang J, Luo YT, Wang P, Wei Y, Zhou YR. Fault diagnosis of rotating machinery under complex conditions based on multi-scale convolutional neural networks[C]//Journal of Physics: Conference Series. IOP Publishing, 2023, 2658(1): 012038. DOI: 10.1088/1742-6596/2658/1/012038
17. Zhang HC, Shi PM, Han DY, Jia LJ. Research on rolling bearing fault diagnosis method based on AMVMD and convolutional neural networks[J]. Measurement, 2023, 217: 113028. DOI: 10.1016/j.measurement.2023.113028
18. Peng DD, Wang H, Liu ZL, Zhang W, Zuo MJ, Chen J. Multibranch and multiscale CNN for fault diagnosis of wheelset bearings under strong noise and variable load condition[J]. IEEE Transactions on Industrial Informatics, 2020, 16(7): 4949-4960. DOI: 10.1109/tii.2020.2967557
19. Huang NT, Chen QZ, Cai GW, Xu DG, Zhang L, Zhao WG. Fault diagnosis of bearing in wind turbine gearbox under actual operating conditions driven by limited data with noise labels[J]. IEEE Transactions on Instrumentation and Measurement, 2020, 70: 1-10. DOI: 10.1109/tim.2020.3025396
20. Liang PF, Wang WH, Yuan XM, Liu SY, Zhang LJ, Cheng YW. Intelligent fault diagnosis of rolling bearing based on wavelet transform and improved ResNet under noisy labels and environment[J]. Engineering Applications of Artificial Intelligence, 2022, 115: 105269. DOI: 10.1016/j.engappai.2022.105269
21. Hu BB, Tang JH, Wu JM, Qing JJ. An attention EfficientNet-based strategy for bearing fault diagnosis under strong noise[J]. Sensors, 2022, 22(17): 6570. DOI: 10.3390/s22176570
22. Wang X, Qin Y, Wang Y, Xiang S, Chen HZ. ReLTanh: An activation function with vanishing gradient resistance for SAE-based DNNs and its application to rotating machinery fault diagnosis[J]. Neurocomputing, 2019, 363: 88-98. DOI: 10.1016/j.neucom.2019.07.017
23. Zheng QM, Tan D, Wang FH. Improved convolutional neural network based on fast exponentially linear unit activation function[J]. IEEE Access, 2019, 7: 151359-151367. DOI: 10.1109/access.2019.2948112
24. Lin GF, Shen W. Research on convolutional neural network based on improved Relu piecewise activation function[J]. Procedia computer science, 2018, 131: 977-984. DOI: 10.1016/j.procs.2018.04.239
25. Chang SY, Zhang Y, Han W, Yu M, Guo XX, Tan W, Cui XD, Witbrock M, Hasegawa-Johnson M, Huang TS. Dilated recurrent neural networks[J]. Advances in Neural Information Processing Systems, 2017, 30. DOI: arxiv-1710.02224
26. Kuo CCJ. Understanding convolutional neural networks with a mathematical model[J]. Journal of Visual Communication and Image Representation, 2016, 41: 406-413. DOI: 10.1016/j.jvcir.2016.11.003
27. Yu JH, Lin Z, Yang JM, Shen XH, Lu X, Huang TM. Free-form image inpainting with gated convolution[C]//Proceedings of the IEEE/CVF International Conference on Computer Vision. 2019: 4471-4480. https://doi.org/10.1109/ICCV.2019.00457

28. Case Western Reserve University Bearing Data Center; 2018. Available at: https://csegroups.case.edu/bearing data center/pages/download-data-file.
29. Shao ZH, Li WQ, Xiang H, Yang SX, Weng ZQ. Fault diagnosis method and application based on multi-scale neural network and data enhancement for strong noise[J]. Journal of Vibration Engineering & Technologies, 2024, 12(1): 295-308. DOI: 10.1007/s42417-022-00844-x
30. Chao ZQ, Han T. A novel convolutional neural network with multiscale cascade midpoint residual for fault diagnosis of rolling bearings[J]. Neurocomputing, 2022, 506: 213-227. DOI: 10.1016/j.neucom.2022.07.022
31. Li F, Wang LP, Wang DC, Wu J, Zhao HJ. An adaptive multiscale fully convolutional network for bearing fault diagnosis under noisy environments[J]. Measurement, 2023, 216: 112993. DOI: 10.1016/j.measurement.2023.112993
32. Wang Q, Xu FY. A novel rolling bearing fault diagnosis method based on adaptive denoising convolutional neural network under noise background[J]. Measurement, 2023: 113209. DOI: 10.1016/j.measurement.2023.113209